JOURNAL OF MATERIALS SCIENCE **34** (1999) 3263–3273

Fatigue-life prediction of SiC particulate reinforced aluminum alloy 6061 matrix composite using AE stress delay concept

D. SHAN, H. NAYEB-HASHEMI
Department of Mechanical, Industrial and Manufacturing Engineering, Northeastern University, Boston, MA 02115
E-mail: hamid@coe.neu.edu

A study of the residual fatigue life prediction of 6061-T6 aluminum matrix composite reinforced with 15 vol % SiC particulates (SiC_p) by using the acoustic emission technique and the stress delay concept has been carried out. Fatigue damages corresponding to 40, 60 and 80% of total fatigue life were stimulated at a cyclic stress amplitude. The specimens with and without fatigue damage were subjected to tensile tests. The acoustic emission activities were monitored during tensile tests. It was found that a lower stress level was required to reach a specified number of cumulative AE events for specimens fatigued to higher percentage of the fatigue life. This stress level is called stress delay. Approximately a linear relation was found between stress delay and fatigue damage. Using the procedure defined in this study, the residual fatigue life can be predicted by testing the specimen in tension and monitoring the AE events. The number of the cumulative AE events increased exponentially with the increase of strain during tensile tests. This exponential increase occurred when the material was in the plastic regime and was attributed mainly to SiC particulate/matrix interface decohesion and linkage of voids. In high cycle fatigue, it was observed that the residual tensile strengths of the material did not change with prior cyclic loading damages since the high cycle fatigue life was dominated by the crack initiation phase.

1. Introduction

In recent years, the metal matrix composites (MMCs) reinforced by ceramic particulates have received a wider acceptance as structural materials in design of many components. These materials can be manufactured by either casting or a standard powder metallurgy technique. Aluminum-based particulate reinforced MMCs have a high specific strength and stiffness, which make them attractive materials for automotive and aerospace industries. Since these materials are being used where they are subjected to cyclic loading, it is important to predict the fatigue life and understand their damage mechanism using a nondestructive evaluation technique. The acoustic emission technique is found to be very useful to monitor and collect the information about the damage in materials.

Baram and Rosen [1–3] monitored acoustic emissions from aluminum alloy 2024-T3 and 7076-T6 during low cycle fatigue experiments. The extreme AE peak amplitudes were treated by order statistics. It was found that the extreme AE peak amplitudes to be extremely distributed and a formal relation existed between the extreme AE peak amplitudes and the extreme fatigue crack propagation rates. They concluded that, by treating the extreme value among the AE amplitudes collected during a specific interval of the fatigue life with an order statistics procedure, the number of cycles left until failure can be evaluated.

Fang and Berkovits [4, 5] studied fatigue damage accumulation by acoustic emission on Incoloy 901 and the cumulative fatigue damage was revealed by integration of the cumulative ringdown counts. Three damage phases were recognized in the fatigue: (i) initial elastic softening, (ii) crack incubation and initiation, (iii) crack propagation. A model was developed to define this three stages based on the AE activity due to dislocations and from cyclic hardening/softening. To assess fatigue damage accumulation, a damage parameter was defined as the ratio of total ringdown counts at a given moment to the sum of ringdown counts occurring until failure. An expression for this damage parameter in term of fatigue life was obtained.

Bhat *et al.* [6] studied the fatigue behavior of glass fiber reinforced plastic. The specimens were subjected to a cyclic load level while the acoustic emissions were monitored. The data were classified using pattern recognition techniques. Each of the AE data files collected from individual tests under fatigue loading was subjected to clustering by the threshold *k*-means algorithm. It was found that the different stages of fatigue process were marked with different clusters of AE signals. It was concluded that a measure of these categories

of AE events at any instance can yield a measure of the cumulative damage undergone by the material and can help in prediction of residual life.

Despite these investigations, there are limited studies using these techniques to evaluate residual fatigue life of particulate reinforced MMCs and identify the sources of acoustic emission. Niklas *et al.* [7] studied the acoustic emission during fatigue crack propagation in AA6061 reinforced with 5, 10 and 20 wt % SiC_p. The fatigue tests were done on single edge notched specimens. It was found that the acoustic emissions increased with the addition of SiC particles. Furthermore, cumulative number of acoustic emission events was also increased with increase in the fatigue crack growth rate.

To use the above techniques to predict the residual fatigue life, it is necessary to monitor the acoustic emission when the specimen is under cyclic loading. This is time consuming and it may be difficult to eliminate extraneous background noise. Background noise is particularly serious in fatigue for two reasons: the AE signal level in fatigue is relatively low, while the cyclic loading process is inherently noisy.

The AE [parameter] delay concept introduced by Williams and Lee [8] could be an alternative to avoid those difficulties with background noise. A specimen after suffering a certain damage level was subjected to tensile load and AE activity was collected. As illustrated in Fig. 1, the AE [parameter] delay was defined as the parameter value that was required to produce a specified low baseline level of cumulative AE measure. The [parameter] can be load, stress, strain, displacement, time, temperature, load cycle, etc.

The purpose of this paper is to study the fatigue properties of SiC particulate reinforced 6061-T6 aluminum alloy. The concept of stress delay is used to explore its feasibility in predicting the residual fatigue life of SiC particulate reinforced Al matrix composites nondestructively using acoustic emission method, and identifying the damage mechanisms.

2. Experimental

2.1. Material

The material tested was 6061-T6 aluminum alloy reinforced with 15% volume fraction SiC particulates. The nominal particulate size is 5 μm. The materials were provided by the Army Material Research and Technology in Watertown, MA. The materials were manufactured by ALCOA by blending atomized aluminum alloy powders with SiC_p, compacting by cold isostatic pressing, densifying to roughly theoretical density by degassing and vacuum hot pressing, and finally extruding into plates with thickness 2.54 mm.

Al_4C_3 formation is one of the main reactions observed in Al-SiC systems. Although a small reaction zone is desirable for bonding particle to matrix, its over growth is known to significantly degrade the properties of the material [9]. The extent of the reactions depends on alloy chemistry and processing conditions, particularly temperature and time. Preliminary investigation of the as received composites showed no formation of Al_4C_3. This is the result of the relatively short duration and low temperature involved during processing of composite.

2.2. Fatigue and tensile test

An Instron 1350 Material Testing System was used to conduct fatigue and tensile test. The specimens were dog-bone shape with a cross section 6.35 $\times$ 2.44 mm and a gage length of 25.4 mm, Fig. 2.

In the tensile test of undamaged specimen, the ultimate strength and yield strength of the material was

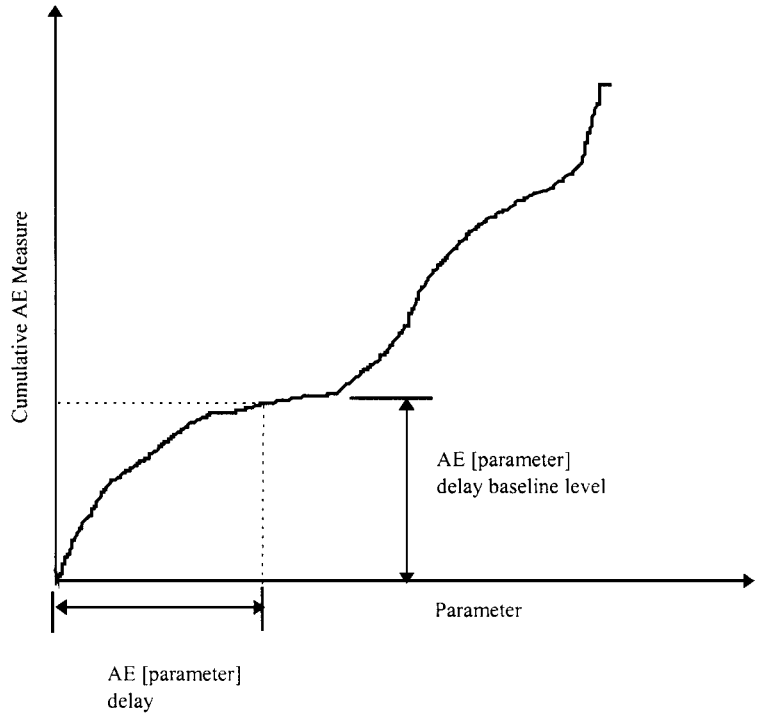

Figure 1 Schematic diagram of cumulative event vs. a parameter showing the concept of AE [parameter] delay [8].

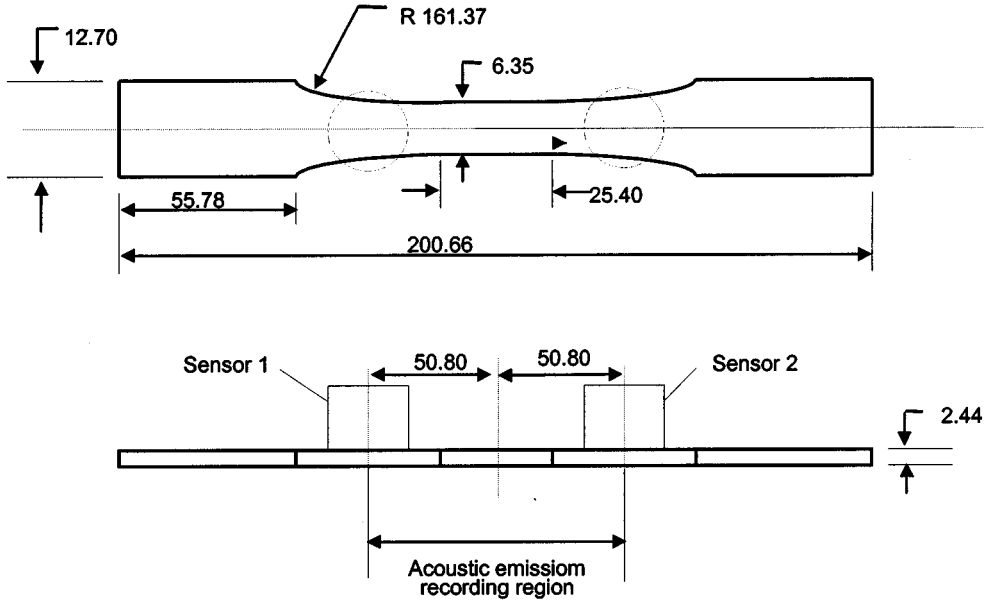

Figure 2 Schematic diagram of the fatigue and tensile specimens and AE sensor placement, dimension in mm.

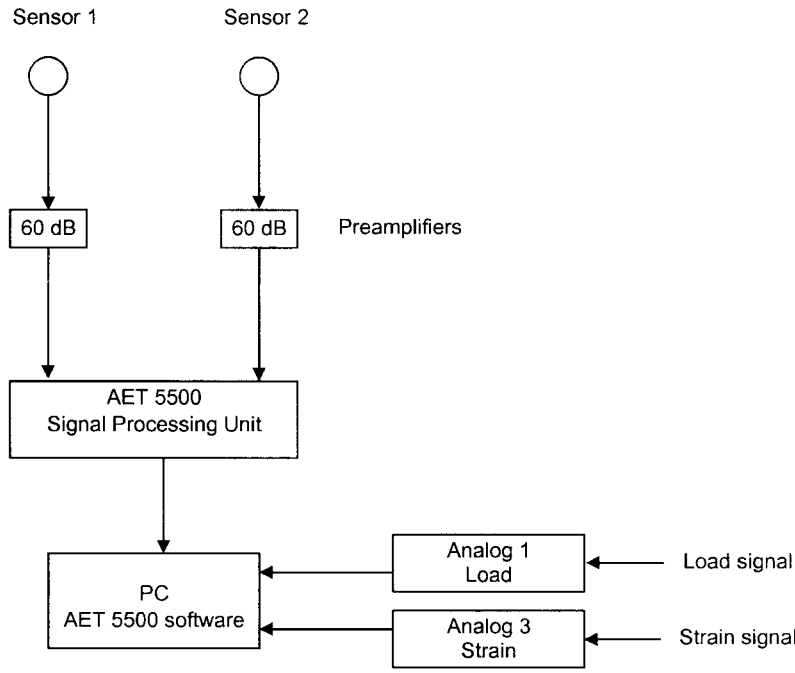

Figure 3 Schematic diagram of the acoustic emission experimental setup.

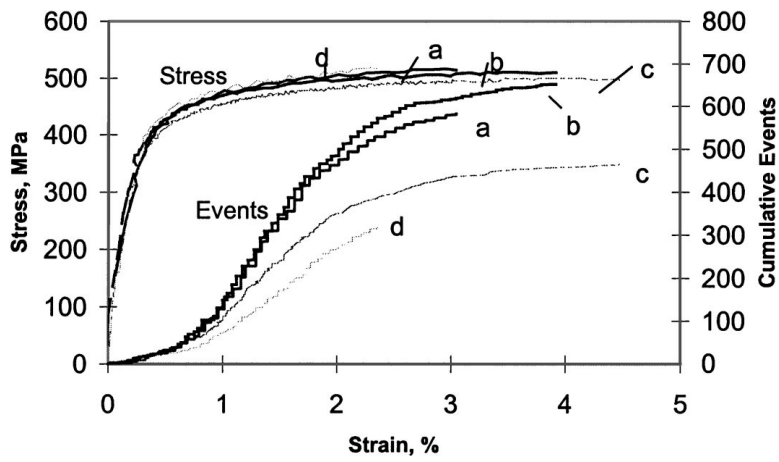

Figure 4 Stress-strain curves and cumulative events vs. strain of the as received specimen and specimens with different fatigue damage levels: (a) as received, (b) 40% damaged, (c) 60% damaged and (d) 80% damaged.

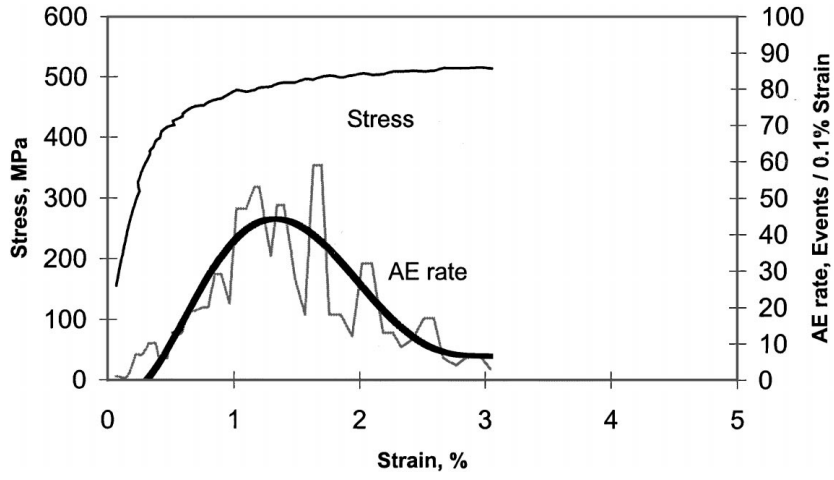

Figure 5 Acoustic emission event rate (ΔEvents)/ΔStrain in an as received specimen.

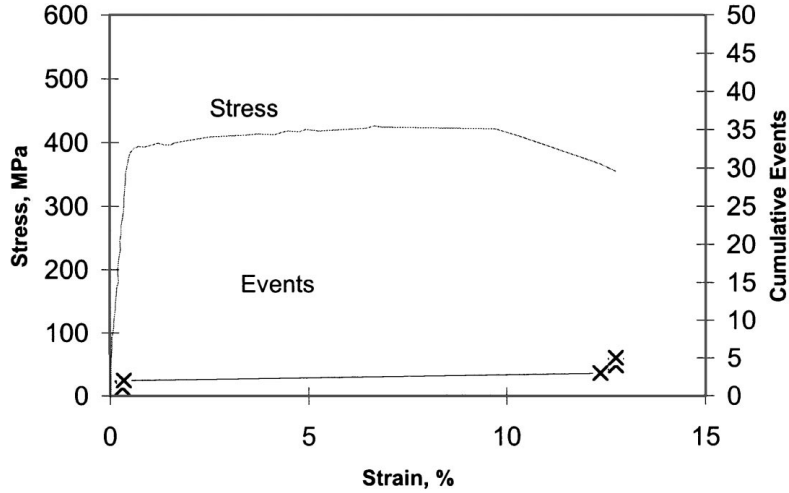

Figure 6 Stress and cumulative events vs. strain for the matrix material, 6061-T6 aluminium alloy.

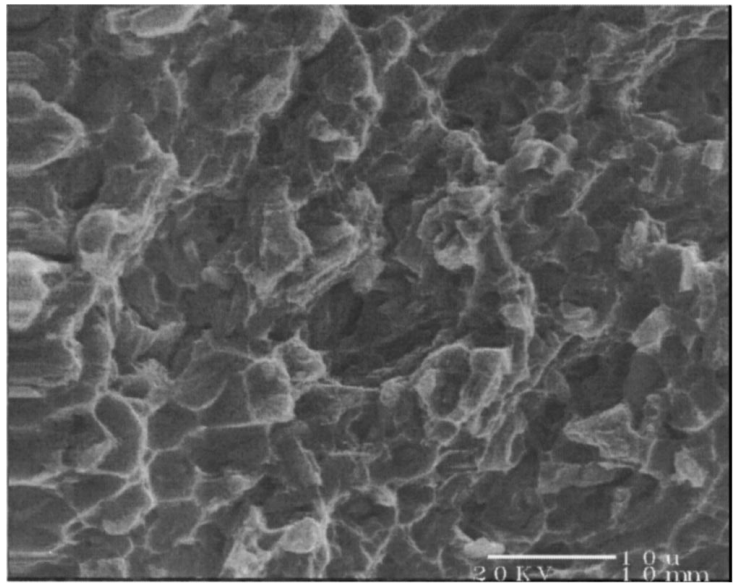

Figure 7 Tensile fracture surface of an as received specimen, showing voids formation.

found to be 514 and 410 MPa respectively. The AE activities were monitored during the test.

In fatigue experiments, specimens were subjected to a constant cyclic stress amplitude at cyclic stress ratio ($\sigma_{min}/\sigma_{max}$) of 0.1 and frequency of about 6 Hz. The maximum stress was 287 MPa, which was about 70% of yield strength of the material. The fatigue life of the material at this cyclic stress range was 1,802,300 cycles. To stimulate fatigue damage of 40, 60 and 80%, a number of specimens were subjected to fatigue with the

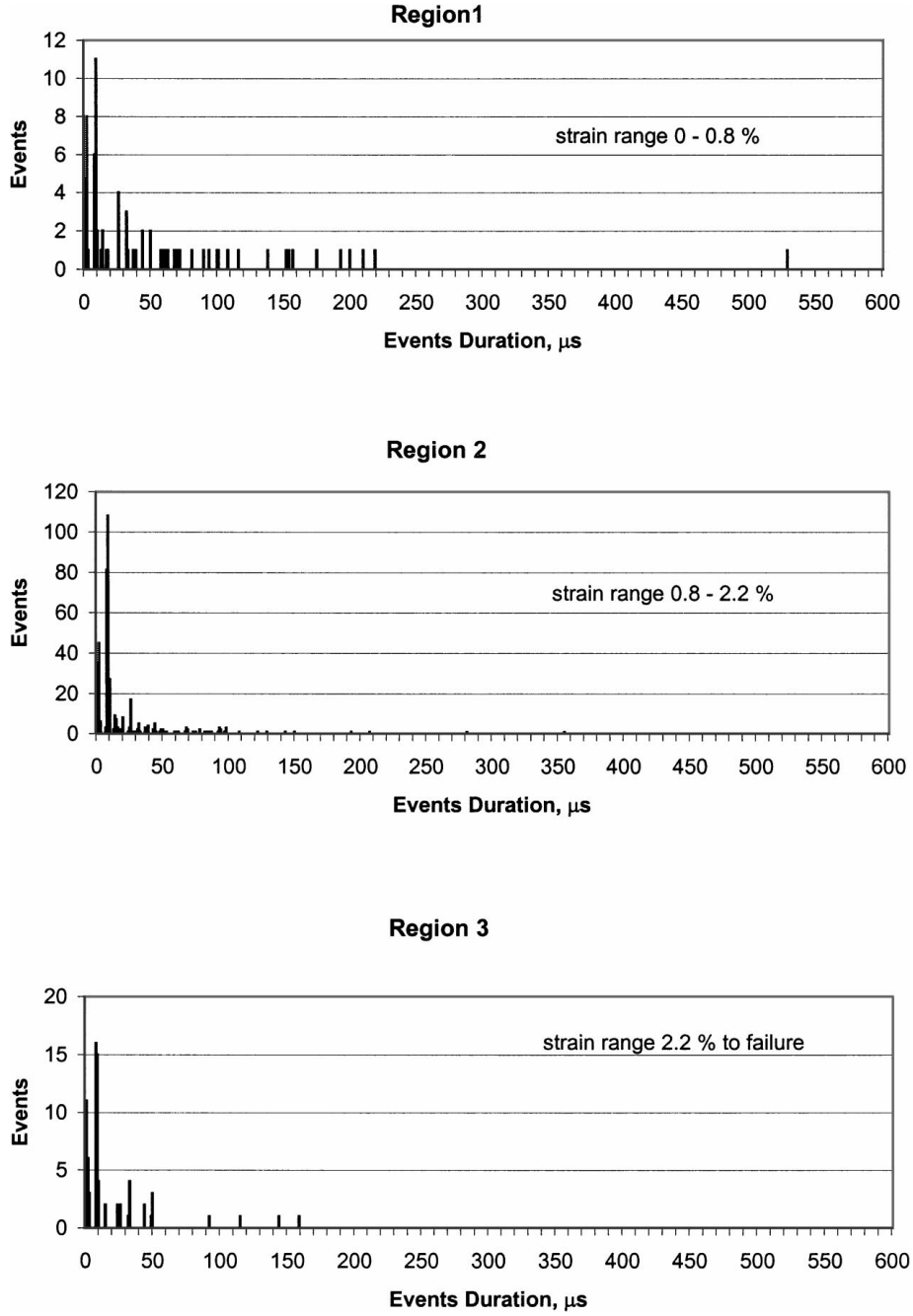

Figure 8 Distribution of events by event duration in 3 regions in as received specimen.

same fatigue parameters up to 720,920, 1,081,380 and 1,441,840 cycles respectively. After fatigue damage, specimens were subjected to tensile tests. The residual tensile strengths of the material were evaluated and the acoustic emissions were monitored during the tensile tests. Unreinforced 6061-T6 aluminum alloy was also subjected to tensile test. The AE activity during the test was monitored for comparison.

2.3. Acoustic emissions monitoring

Acoustic emissions were monitored with an AET 5500 computerized system. Two 175 kHz piezoelectric sensors were clamped to the gage section of the specimens with a spring clamp system. The sensors were coupled to specimens with a couplant. Two 60 dB preamplifiers were used which with 10 dB system amplification provided the total system gain of 70 dB. Teflon-rubber sheets were used between the specimens and the grips to reduce the noise level from the system. The band pass filters in the preamplifiers was of 125–250 kHz (FL12) and floating signal threshold setting of 0.3 V was used to eliminate the background noise. Two sensors were placed in linear location array. The tests were run in time-difference module TDM. The lead pencil fractures were used to simulate AE signals in the calibration of each test, according to the ASTM standard [10]. A region between two sensors was specified from which all AE data was collected and analyzed, Fig. 3. The other unwanted signals outside of this region were rejected by the software.

3. Results and discussions

In the tensile tests of this study, the number of cumulative AE events increased exponentially after material yielding. However, this increase slowed down before the final failure except for the specimens with the 80%

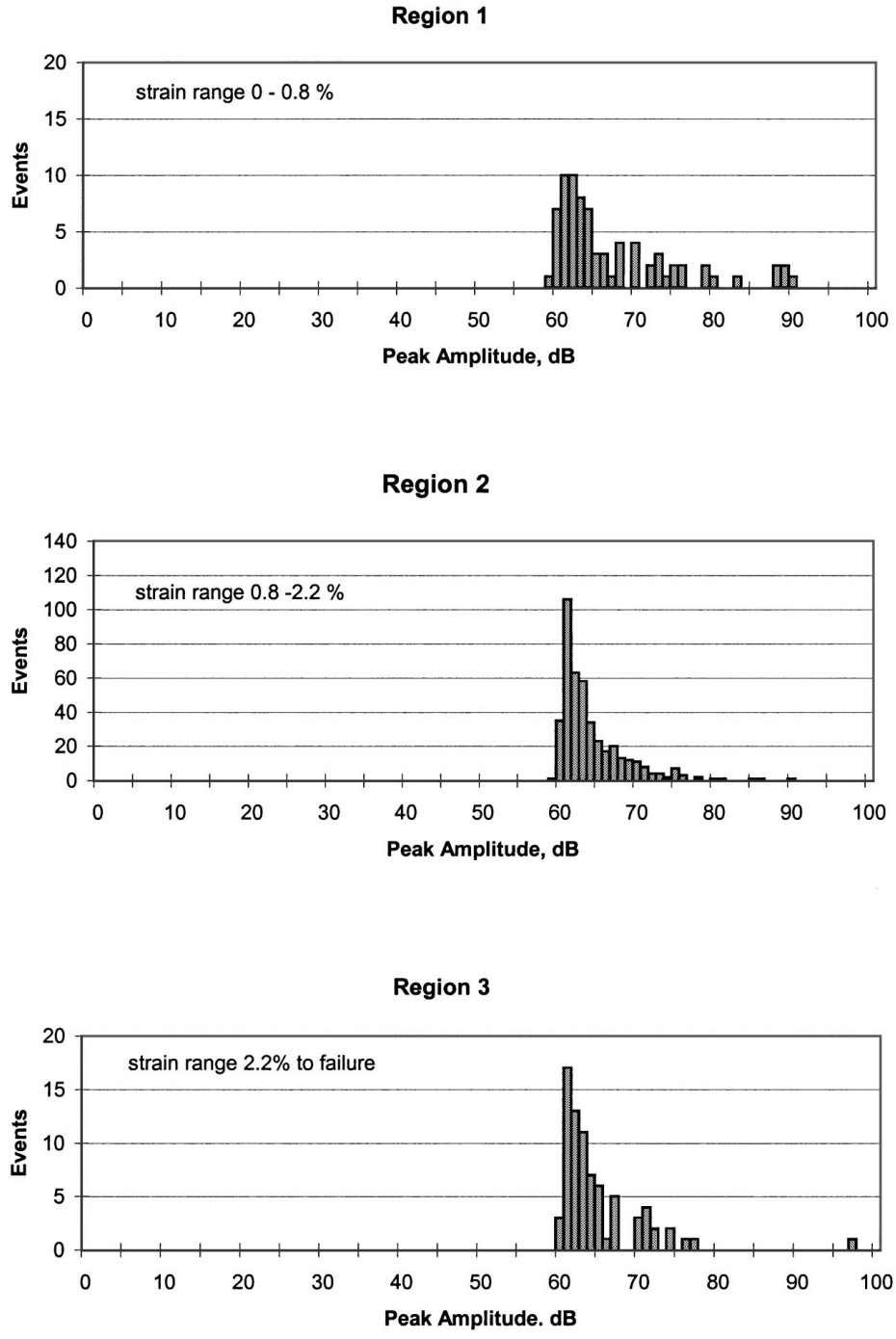

Figure 9 Distribution of events by peak amplitude in 3 regions in as received specimen.

fatigue damage, Fig. 4. The rate of the AE activity defined as Δ(Events)/Δ(Strain) is shown in Fig. 5. Fig. 5 shows that the maximum events rate occur well into the plastic deformation regime of the material. The AE rate is then subsequently reduced until the specimen fails. These results are very similar to those reported by Heiple *et al.* [11], Scruby *et al.* [12, 13], Cousland and Scala [14–16] and McBride *et al.* [17], and differ from those reported by Mummery *et al.* [18] who found a constant event rate when testing aluminum alloy 1070 and 5050 reinforced with SiC particulates.

There are many suggested mechanisms for the observed acoustic emission activity in aluminum alloys and particulate reinforced aluminum alloys. While Heiple *et al.* [11] and Scruby *et al.* [12, 13] relate the high rise in AE activity on the onset of material yielding to dislocation motion, Cousland and Scala [14–16] and McBride *et al.* [17] relate it to fracture of large inclusions in the material. Cousland and Scala studied AA 7075, 7050, 2024, 2124 and 6061-T651. The AE activity under both monotonic and cyclic loading was found to depend on the inclusion size and the number of inclusions. In AA 6061-T651, which has fewer and smaller inclusions than the others, fewer AE activity was observed. Furthermore no AE was detected during compression deformation. McBride *et al.* did not detected AE from inclusion-free AA 7075-T6 during slow fatigue crack growth. Therefore, the AE events were attributed to the inclusion fracture.

Based on our experimental observations, the initial exponential increase of the acoustic emission events were related to the numerous void nucleation,

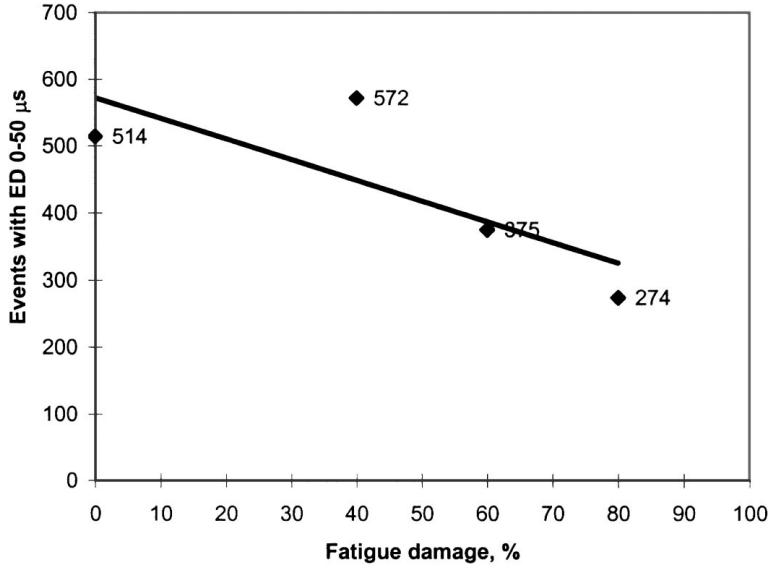

Figure 10 Number of the events with event duration 0–50 microseconds vs. fatigue damage.

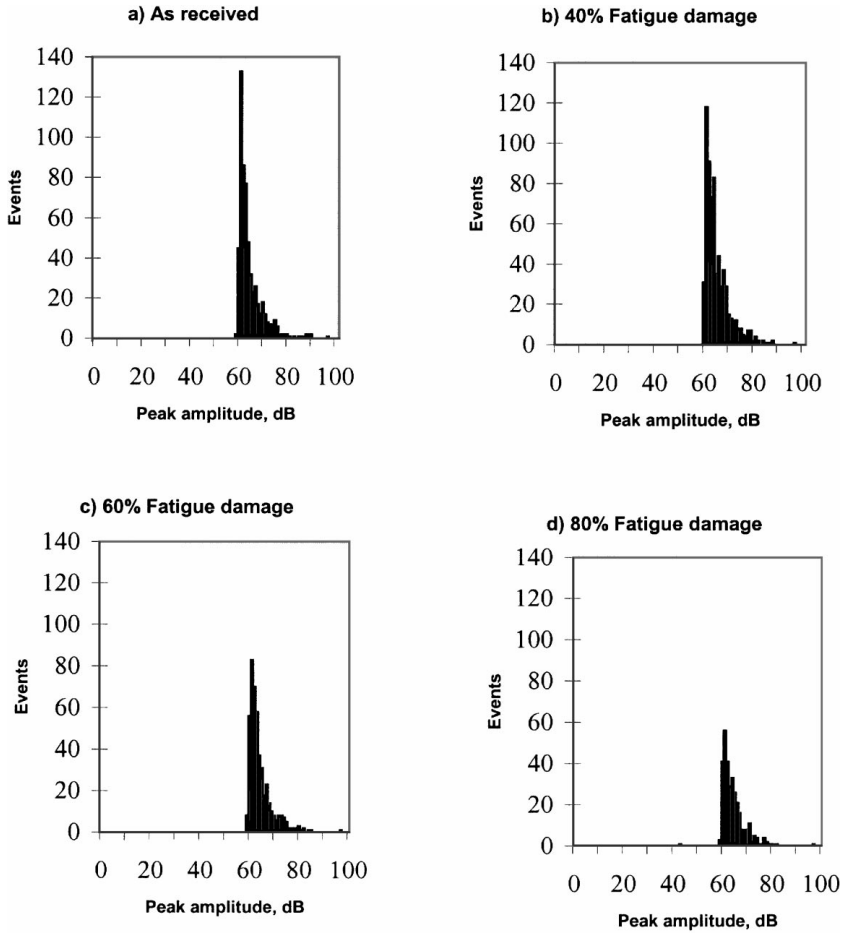

Figure 11 Distribution of events by peak amplitude, for specimens with different damage levels.

particle/matrix debonding and the linkage of voids. The events are then slowed down as the number of particle/matrix debonding reduces. These conclusions are justified as follows. The AE activity of the composite initiated well into the plastic regime of the material. Therefore, dislocation activity could not be considered as an AE source for this group of the composites. The AE activity from dislocations depends on the dislocation density and distance dislocations can move. It has been shown [11–13] that the AE activity corresponding to dislocation motion increase upon material yielding and slowed down due to dislocation pinning. Furthermore, AE activity of unreinforced 6061-T6 under the same experimental condition was evaluated and a very few AE events were detected during tensile test, Fig. 6. The AE activity of our composite also could not be related to the inclusion fracture. The micromechanisms of the failure were studied using a scanning

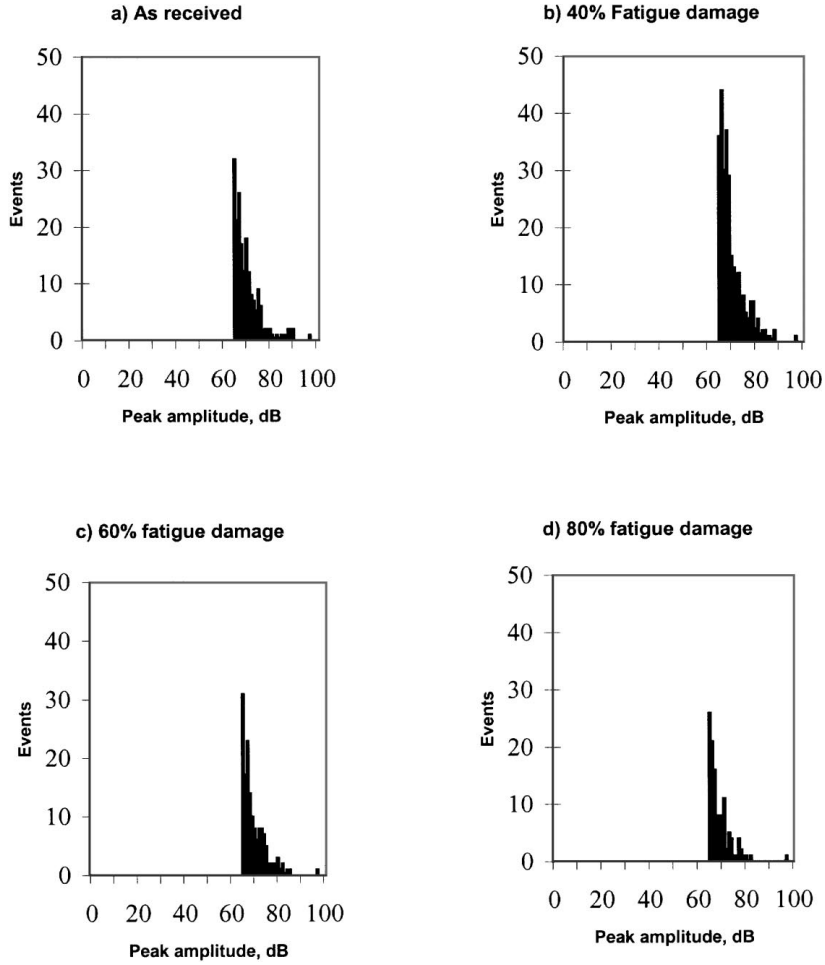

Figure 12 Distribution of events with 65–100 dB peak amplitude by peak amplitude, for specimens with different damage levels.

electron microscope, Fig. 7. The fracture surface was covered with voids and only with a very few particles fractured.

These results are consistent with those reported by Mummery *et al.* [18] and Niklas *et al.* [7], who related the AE activity in a SiC_p reinforced aluminum alloy to the rate of the void nucleation at the particle/matrix interface and the growth of the voids. Void nucleation was observed from onset of plastic deformation. Local failure processes in the matrix were shown to promote void coalescence and dominate the ductility.

The interface region in a given composite determines the ultimate properties of the composite. A strong interfacial bond is usually achieved by the formation of an adequately thin layer at the interface under optimum wetting conditions of the molten metal on the reinforcement. However, SiC exhibits a poor wettability by a molten matrix. Addition of alloying elements, such as lithium and magnesium, has proved to be an effective method to enhance the wettability of the reinforcement by the molten matrix. Some of these alloying elements can react with the reinforcement to form chemical reaction products at the interface. Carotenuto *et al.* [19] showed that the SiC-Al interface is chemically stable at temperatures below 650 °C. At higher temperature SiC reacts with aluminum leading to formation of Al_4C_3 and Si at the particle/matrix interface. Wang *et al.* [20] observed formation of magnesium aluminate $MgAl_2O_4$, a spinel at the interface of A356 reinforced with 15 vol % SiC_p. In addition, fractographic observation by Vedani *et al.* [21] on the same material indicated preferential cracking of the reinforcement particles in the underaged composites, whereas overageing led to more frequent interface debonding. The structure of the interface is also found to be related to the processing method of the composite. Romero *et al.* [22] found the interface in a powder metallurgy processed was relatively clean of precipitates or void.

Since our composites were manufactured by powder metallurgy techniques, we believe the interface was not strong, leading to the particle/matrix debonding in tensile test. This further confirms that the AE activities are due to void formation and linkage of the voids. The distributions of events by the peak amplitude and by event duration were analyzed by grouping AE data for each test into three regions: the early activity (strain range of 0–0.8%), exponential rise (strain range of 0.8–2.2%), and final slow down region (strain range of 2.2% to failure) (see Figs 8 and 9). Figs 8 and 9 show that distribution of events are similar in the three regions. This may indicate that the same mechanisms are operating in all three regions. Furthermore, majority of the activity in each region corresponds to events with small event duration (less than 50 μs) and 60–64 dB peak amplitudes. This again confirming that a single dominating mechanism is responsible for the composite failure. The distribution of events apparently did not change by exposing specimens to fatigue. However, the number of activity reduced with the fatigue exposure, Fig. 10.

TABLE I Residual tensile strength after fatigue damage

Specimen condition	No damage	40% damage	60% damage	80% damage
Ultimate strength	514 MPa	510 MPa	500 MPa	517 MPa

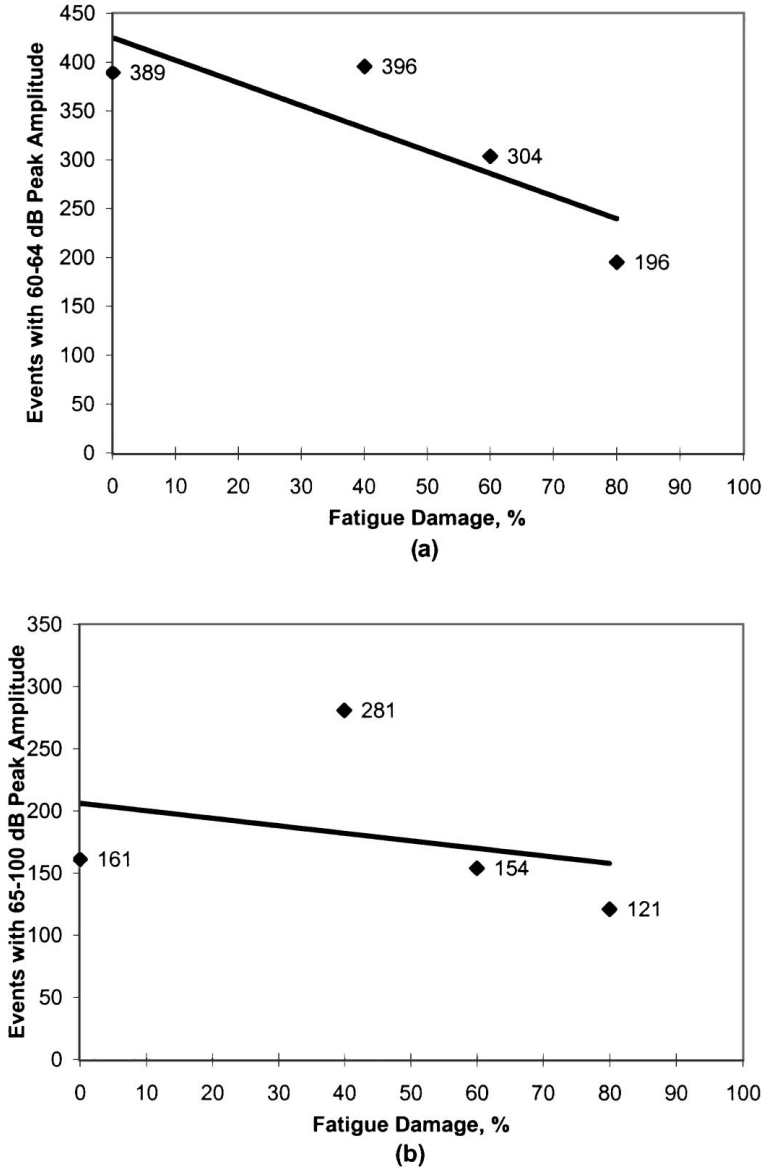

Figure 13 (a) Events with 60–64 dB peak amplitudes vs. fatigue damage and (b) Events with 65–100 dB peak amplitudes vs. fatigue damage.

Comparison of the tensile strength of the specimens with different fatigue damage level showed that the fatigue damage almost did not affect the tensile strength of the material (Table I). This agrees with the high cycle fatigue mechanism. In high cycle fatigue, the fatigue life is dominated by the crack initiation period and cracks are only initiated at the final stage of the fatigue life. At 40, 60 or 80% damage level, cracks either have not initiated or initiated cracks are within statistical size of the defects in the material, so the tensile strength of the material did not change significantly due to prior exposure of specimens to cyclic loading.

The contribution of the reinforcement to crack initiation depends on the reinforcement volume fraction, shape, size and interfacial bond strength. A number of studies on the fatigue crack initiation in SiC_p reinforced aluminum alloys have shown that the cracked SiC_p and SiC/Matrix interface are the preferential crack initiation sites [23]. Skolianos [24] studied the fatigue behavior of SiC_p reinforced Al-4.5%Cu-1.5%Mg composite. Metallographic examination of crack nucleation and growth carried out on electropolished specimens indicated that SiC particulates appear to have a significant stress-raising effect on the formation of slip bands and cracks. During high cycle fatigue, the stress is not high enough to initiate crack quickly. Even cracks were initiated, their sizes were small. The fracture surface evaluation of the fatigued specimens indeed indicated of no crack growth regions. The detected AE activity therefore are not due to any crack growth.

The distribution of events by peak amplitude for specimens with different percentage of damage is shown in Fig. 11. The events with 60–64 dB peak amplitudes were subtracted from the total distribution

in Fig. 12. Fig. 13 shows that the number of events with 60–64 dB peak amplitudes reduces linearly with the increase of fatigue damage while the number of the events with 65–100 dB peak amplitudes had no obvious change with increase of fatigue damage. If the events corresponding to the particle/matrix debonding are assumed to have peak amplitude in the range of 60–64 dB, the remaining distribution could be assumed to be due to linkage of voids. The specimen could be assumed to fail upon having a critical number of debonded particles. This critical number could be reached by a combination of tensile load and prior fatigue damage. The AE activity due to the void linkage should therefore be independent of the fatigue damage status.

The results also show a linear relation between the residual fatigue life and the stress required to produce a specific cumulative events, Figs 14–16. Therefore, acoustic emission could be used effectively to predict the residual fatigue life of this group of composites.

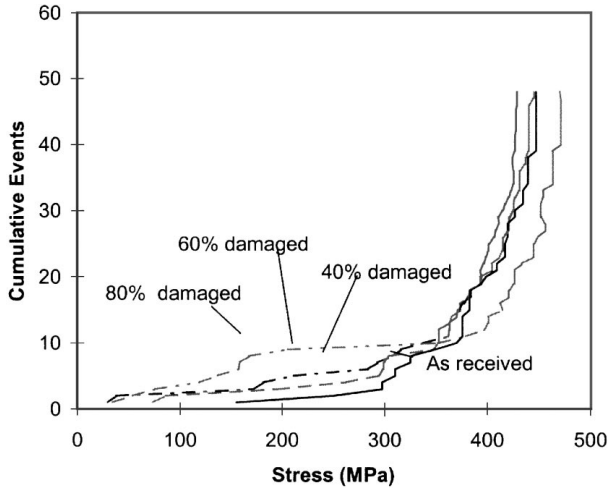

Figure 14 Cumulative AE events vs. stress for as received specimen and specimens with 40, 60 and 80% fatigue damage (specimens load up to total cumulative events of 50).

4. Conclusions

Acoustic emission activity of a SiC_p reinforced 6061-T6 aluminum alloy was monitored during tensile tests in the as received specimens and after specimens were subjected to cyclic fatigue loading for a number of cycles. It was found,

(1) The AE activity rises quickly once the material is well in the plastic regime. The activity was related to the particle/matrix debonding and linkage of voids.

(2) The tensile failure was postulated to occur in a material having a critical number of debonded particles. The number of debonded particles increased with the increase of the fatigue damage. The subsequent AE activity during tensile tests thus decreased with the fatigue damage.

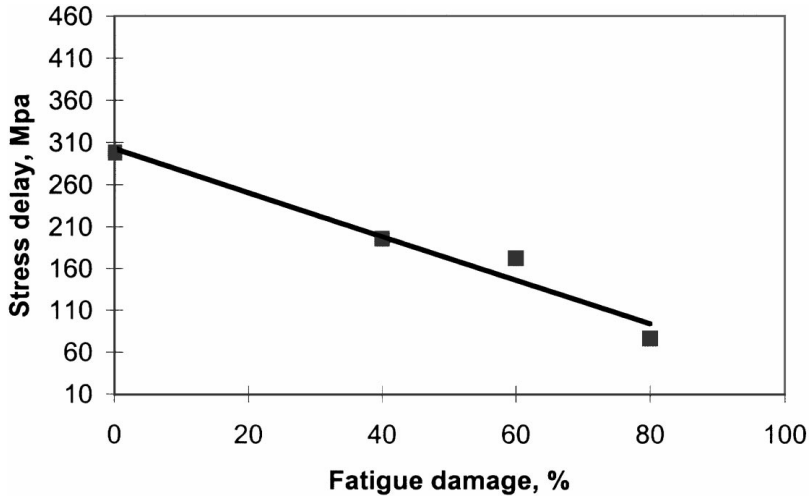

Figure 15 Stress delay vs. fatigue damage for the cumulative AE events of 3.

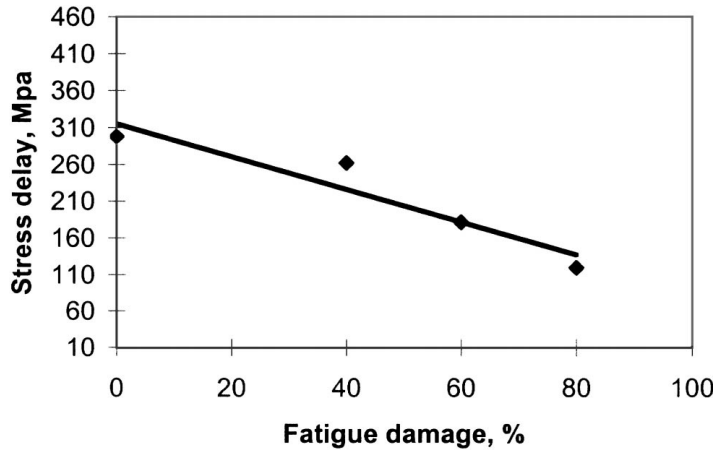

Figure 16 Stress delay vs. fatigue damage for the cumulative AE events of 4.

(3) There was little difference in the AE activity of the specimens in the second stage of damage, which is the linkage of voids.

(4) Linear relations were found between the number of events with 60–65 dB peak amplitude and the residual fatigue life, and between stress required to produce a specific cumulative events and the residual fatigue life.

(5) In high cycle fatigue, the residual tensile strength of the SiC_p reinforced 6061-T6 aluminum alloy composite was found not to be affected by the prior cyclic loading. The crack initiation period dominated the life of the composite in the high cycle fatigue regime.

References

1. J. BARAM and M. ROSEN, *Eng. Fracture Mech.* **15** (1981) 477–486.
2. *Idem., ibid.* **15** (1981) 487–494.
3. J. BARAM, *ibid.* **19** (1984) 181–185.
4. D. FANG and A. BERKOVITS, *Transaction of the ASME* **117** (1995) 200–208.
5. *Idem., Fatigue and Fracture of Eng. Mater. & Structure* **7**(9) (1994) 1057–1067.
6. M. R. BHAT, M. A. MAJEED and C. R. L. MURTHY, *NDT & E International* **27**(1) (1994) 27–32.
7. A. NIKLAS, L. FROYEN, M. WEVERS and L. DELAEY, *Metallur. and Materials Transactions A* **26A** (1995) 3183–3189.
8. J. H. WILLIAMS, JR. and S. S. LEE, *Materials Evaluation* **41** (1983) 961–966.
9. L. SALVO, G. L. ESPERANE, M. SUERY and J. G. LEGOUX, *Mater. Sci. Eng.* **A177** (1994) 173–183.
10. ASTM E 976-94, "Standard Guide for Determining the Reproducibility of Acoustic Emission Sensor Response" (ASTM, Philadelphia, PA) 19103.
11. C. R. HEIPLE, S. H. CARPENTER and M. J. CARR, *Metal Science* **15** (1981) 587–598.
12. C. B. SCRUBY, H. N. G. WADLEY, K. RUSHBRIDGE and D. STOCKHAM-JONES, *ibid.* **15** (1981) 599–609.
13. C. B. SCRUBY and H. N. G. WADLEY, *Philosophical Magazine A* **44**(2) (1981) 249–274.
14. S. McK. COUSLAND and C. M. SCALA, *Metal Science* **15** (1981) 609–614.
15. *Idem., J. Mater. Sci. Lett.* **3** (1984) 268–270.
16. *Idem., Mater. Sci. Eng.* **57** (1983) 23–29.
17. S. L. McBRIDE, J. W. MACLACHLAN and B. P. PARADIS, *J. Nondestructive Evaluation* **2** (1981) 35–41.
18. P. M. MUMMERY, B. DERBY and C. B. SCRUBY, *Acta Metall. Mater.* **41**(5) (1993) 1431–1445.
19. G. CAROTENUTO, A. GALLO, L. NICOLAS, *J. Mater. Sci.* **29** (1994) 4967–4974.
20. N. WANG, Z. WANG and G. C. WEARTHERLY, *Metall. Trans.* **23A** (1992) 1423–1430.
21. M. VEDANI, E. GARIBOLDI, G. SILVA and C. DIGREGORIO, *Mater. Sci. and Tech.* **10** (1994).
22. J. C. ROMERO, L. WANG and R. J. ARSENAULT, *Mater. Sci. and Eng. A* **212** (1996) 1–5.
23. S. KUMAI, J. E. KING and J. F. KNOTT, *ibid.* **146** (1991) 317–326.
24. S. SKOLIANOS, *ibid.* **210** (1996) 76–82.

Received 15 October 1997
and accepted 11 November 1998